Journal of Hazardous Materials 188 (2011) 148–155

Contents lists available at ScienceDirect

Journal of Hazardous Materials

journal homepage: www.elsevier.com/locate/jhazmat

# Porous CS monoliths and their adsorption ability for heavy metal ions

Fangqiang Xu[a], Nana Zhang[a], Ying Long[a], Youmiao Si[a], Yu Liu[a,*], Xue Mi[a], Xiaodong Wang[a], Fubao Xing[a], Xiudong You[b], Jianping Gao[a]

[a] School of Science, Tianjin University, Tianjin 300072, PR China
[b] Institute of Medical Equipment, Academy of Military Medical Science, Tianjin 300161, PR China

ARTICLE INFO

*Article history:*
Received 9 September 2010
Received in revised form 21 January 2011
Accepted 21 January 2011
Available online 31 January 2011

*Keywords:*
CS
Porous material
Adsorption
Metal ions

ABSTRACT

Highly porous chitosan (CS) monoliths were prepared by a unidirectional freeze-drying method and the adsorption performance of the monoliths for metal ions in aqueous solution was evaluated. The porous CS monoliths have excellent adsorption for a range of metal ions. The effect of the amount of porous CS monoliths, the pH, the adsorption time, the amount of the cross-linking agent, and the amount of disodium ethylenediamine tetraacetate (EDTA) on the saturated adsorption efficiency (Ade) were determined. The pH had the greatest influence on the adsorption behavior. Under optimal conditions ($C_{Cu^{2+}}$ = 800 mg/L, pH 6, and cross-linking agent = 0.15%) for the CS monoliths, the Ade for $Cu^{2+}$ exceeded 99%, and the saturated adsorption capacity ($Q_s$) reached a value of 141.8 mg/g (2.23 mmol/g) in 4 h. Moreover, the addition of EDTA can both increase the $Q_s$ and shorten the time that achieved the level. If EDTA was added, this level was achieved in 2 h. The porous CS monoliths can be regenerated by soaking them in acid and their Ade is maintained.



## 1. Introduction

Porous materials are an important material because of their unique characteristics and applicability to many different areas including aeronautics, astronautics, and petroleum chemical environmental and tissue engineering. Porous materials with ordered pore structures are required for photonic devices and for the scaffolds used in nerve cells. At present, there are two main methods to prepare porous materials, porogen and non-porogen methods. Foam forming, particle leaching, and freeze-drying are porogen methods [1–4]. The freeze-drying techniques are especially attractive because water can be used as the porogen to prepare the porous materials [5]. However, technologies for preparing porous materials with ordered pore structure are often inconvenient [6–8].

Recently, Ferrer et al. reported a simple and effective way called ice-segregation-induced self-assembly (ISISA) process, or unidirectional freeze-drying method (UFDM) [9]. To date, this is the simplest way to prepare oriented porous materials and the method has been exploited for preparing aligned porous organic [5,10,11,8], inorganic and composite materials [12,13]. Porous materials with ordered pore structures are important for both theoretical studies and technological applications because of their high stability, controllable pore structure and operational convenience [14,15].

Industrial wastewater containing heavy metal ions has generated a great deal of concern as a major threat to human health and several technologies for the efficient removal of ions are being developed. Chemical precipitation or oxidation–reduction methods can be used to convert metal ions into insoluble compounds for subsequent isolation. However, the excessive sludge these methods produce creates additional treatment problems and, if handled improperly, may cause secondary pollution. The use of ion exchange resins to adsorb metal ions is an efficient but expensive approach [16]. Porous materials with high surface areas and connected pores are good candidates for adsorbents. For instance, active carbon or zeolite is often used to adsorb heavy metal ions and other toxic chemicals [17]. Clinoptilolite, a natural zeolite, has been used to remove metal ions from water. Its adsorption capacity depends on the pH and the initial metal ion concentration. Its experimental maximum adsorption capacity for $Cu^{2+}$ and $Pb^{2+}$ is about 90 mg/g and 45 mg/g, respectively [18].

Chitosan (CS), a natural, non-toxic, environmentally friendly polymer, is one of the most promising alternative adsorbents for removing heavy metals from wastewater [19]. It can be easily prepared from chitin and is calculated to have a maximum adsorption capacity of 176 mg/g for $Cu^{2+}$ using a Langmuir adsorption isotherm model [20]. However, its mechanical strength and chemical instability are unfavorable [21], so numerous studies have been devoted to modifying its properties. Cross-linking is an effective way to improve CS's stability [22], and several cross-linking agents such as epichlorhydrin [23], glutaraldehyde [24], and ethyleneglycol digly-

* Corresponding author. Tel.: +86 22 274 041 18; fax: +86 22 274 034 75.
*E-mail address:* tjly@tju.edu.cn (Y. Liu).

0304-3894/$ – see front matter © 2011 Elsevier B.V. All rights reserved.
doi:10.1016/j.jhazmat.2011.01.094

cidyl ether [25] have been used to prepared cross-linked CS beads. Although both mechanical and chemical stability were improved, the adsorption capacity for metal ions decreased as the degree of cross-linking increased, because some of the $-NH_2$ groups are consumed during the cross-linking reaction [26]. Composites are another way to modify CS-based adsorbents [27–29]. Hasan et al. reported that the maximum adsorption capacity for Cu(II) by composite beads of CS coated on perlite was 104 mg/g [30], although the adsorption capacity of prelate itself is not high [31]. To further improve the adsorption properties of CS, various chemical modifications have been investigated such as thiourea-modified CS [32,33], EDTA- and/or DTPA-modified CS [34], $H_2SO_4$ modified CS [35], reactive blue 2 dye-modified CS [36], α-ketoglutaric acid-modified-coated magnetic nanoparticles [37], and $CS_2$-modified CS [38]. For most of these methods, the experimental maximum adsorption capacity of the chemically modified CS is below 100 mg/g, although the calculated values are much higher. For instance, the Langmuir isotherm model predicts adsorptions of up to 225 mg/g for $Cu^{2+}$ and over 340 mg/g for $Pb^{2+}$. Chemical modification can greatly improve adsorption properties, but these methods are usually complex and expensive to carry out. Therefore, efficient adsorbents that are easy to use and inexpensive are desired.

In this study, highly porous CS monoliths were prepared by a unidirectional freeze-drying method [39] and their adsorption capacities for metal ions from aqueous solutions were evaluated.

## 2. Materials and methods

### 2.1. Materials

CS (Mn = 100 K) was purchased from Zhejiang Yuhuan Marine Biochemical Co. Ltd. Glutaraldehyde and copper sulfate were supplied by Beijing Chemical Co. Lead nitrate, acetic acid, concentrated nitric acid, anhydrous ethanol, and ethylenediamine tetraacetate (EDTA) were all from Tianjin Chemical Reagent Co.

### 2.2. Preparation of highly porous CS monoliths

A 1.0 g sample of CS was mixed with 50 mL 0.2 mol/L acetic acid solution in a flask and stirred vigorously to obtain a homogeneous solution. Then 1 mL 5% (g/mL) glutaraldehyde solution as the cross-linking agent was added to the solution with stirring. The mixture was allowed to stand for about 2 h at room temperature, and then it was injected into a PET tube (20 mm in diameter and 50 mm in length). The plastic tube was placed inside a thermally insulated Styrofoam tube, with only the bottom surface of the plastic tube exposed to air. The Styrofoam tube was placed onto the surface of a 6 cm diameter metal disk, which in turn rested on a 6 cm-deep pool of liquid nitrogen for about 10 min to create a uniaxial thermal gradient [40]. As the liquid nitrogen evaporated, the homogeneous CS solution was unidirectionally frozen from the bottom to the top. The solidified CS/water biphase system was then transferred into a freeze-drying vessel (Alpha1-2, Christ, Germany) under vacuum (less than 20 Pa) and freeze-dried for 48 h to obtain porous CS monoliths (a cylinder with 2 cm in diameter and 1.6 cm in height).

The porous CS monoliths were then immersed into an anhydrous ethanol solution containing a small amount of 0.1 mol/L sodium hydroxide. The solution was gently shaken, and then the monoliths were removed and rinsed with pure ethanol. The treated porous CS monoliths were dried in the freeze drier for 6 h, and then stored in a desiccator. They were characterized by scanning electron microscopy (SEM) (JEOL-6700F ESEM, Japan), and their porosity was calculated [41].

### 2.3. Adsorption of porous CS monoliths for $Cu^{2+}$

The porous CS monoliths (0.15% cross-linking agent; pH 6.0) were placed into a 250 mL conical flask containing 100 mL of 50 mg/L copper sulfate solution to allow adsorption to occur at room temperature. A 1 mL aliquot of supernatant was removed each hour for analysis. Each aliquot of supernatant was diluted to 50 mL with distilled water, and then analyzed by flame atomic absorption spectrometry (Solar 969 atomic absorption spectrophotometer, Thermo, U.S.) to determine the concentration of the $Cu^{2+}$ ions. A standard calibration curve was used [42]. The adsorption efficiency (Ad) and adsorption capacity ($Q_t$) were calculated according to the following equations:

$$\mathrm{Ad}(\%) = \frac{C_0 - C_t}{C_0} \times 100 \quad (1)$$

$$Q_t = \frac{(C_0 - C_t)V}{W} \quad (2)$$

where $C_0$ is the initial concentration of copper ions, $C_t$ is the concentration at a given time, $W$ (g) is the weight of the dry porous CS monoliths and $V$ (mL) is the volume of solution. Note that $Q_t$ (mg/g) is the apparent adsorption capacity of the porous monoliths at a given time, and given a long enough adsorption time, it becomes equal to the saturated adsorption efficiency (Ade) and saturation capacity ($Q_s$).

To investigate the effect of EDTA on the adsorption of ions, 25 mL of a 100 mg/L $Cu^{2+}$ solution was mixed with various amounts of an isopycnic EDTA solution to obtain different ratios of EDTA/$Cu^{2+}$. The adsorption measurements of the porous CS monoliths (0.3% cross-linking agent) were carried out for these solutions using the procedures described above.

To explore the adsorption effect of the treated porous CS monoliths (0.3% cross-linking agent), 50 mL aqueous solution of $Cu^{2+}$ metal ions with a concentration of 50 mg/L was poured into a conical flask, and then the treated porous CS monoliths were placed into the solution with mild shaking. The adsorption measurements of the treated porous CS monoliths were carried out as above.

In order to study the adsorption behavior of the porous CS monoliths in a mixture of metal ions, 50 mL aqueous solution of $Cu^{2+}$, $Pb^{2+}$, $Hg^{2+}$, $Cd^{2+}$ and $Ni^{2+}$ metal ions, each with a concentration of 50 mg/L, was poured into a conical flask, and then the porous CS monoliths were placed into the solution with mild shaking. The adsorption behavior of the monoliths at different time intervals was determined by inductively coupled plasma mass spectroscopy (Profile, Leeman Labs, U.S.) [43].

### 2.4. Regeneration and recycling of porous CS monoliths

The porous CS monoliths containing $Cu^{2+}$ were thoroughly rinsed with water and dried under vacuum. Then the dried monoliths were put into 10 mL of nitric acid solution at pH 1 to allow desorption of the $Cu^{2+}$ ions. The concentration of $Cu^{2+}$ in the solution after a certain interval ($C_t^*$) ($C_t^*$ includes $Cu^{2+}$ ions that disengage from the adsorbent during the rinsing step) was determined by flame atomic absorption spectrometry, and the degree of desorption was calculated according to Eq. (3).

$$\mathrm{Desorption}(\%) = \frac{10C_t^*}{Q_s W} \times 100 \quad (3)$$

After the desorption reached completion, the monoliths were removed from solution, rinsed with water and dried in a freeze desiccator.

To investigate the ability of the CS monoliths to be recycled, the regenerated porous CS monoliths were repeatedly subjected to the adsorption and desorption processes.

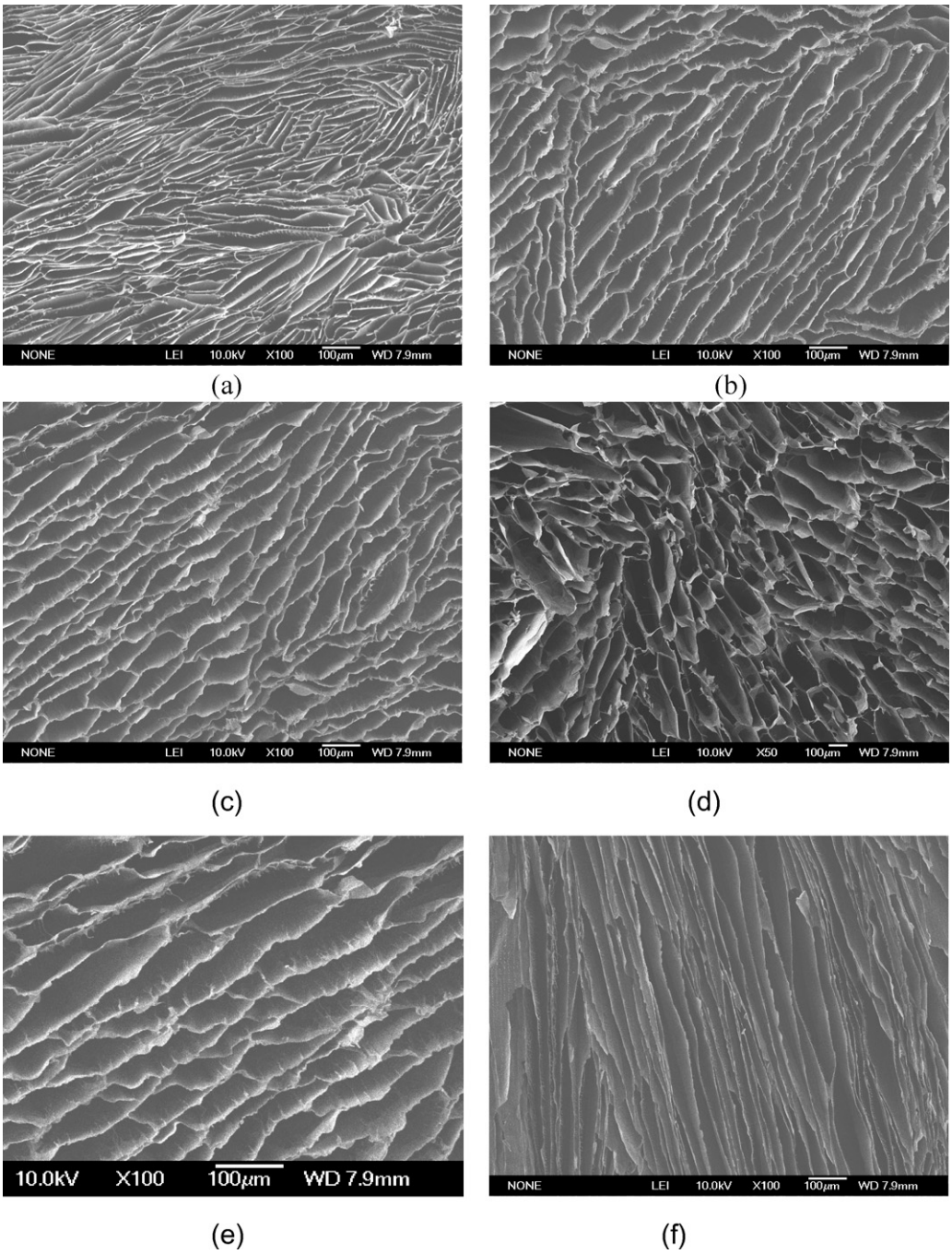


**Fig. 1.** SEM images of the cross-sections of porous CS monoliths with different amounts of cross-linking agent: (a) 0.1%, (b) 0.2%, (c) 0.3%, (d) 0.5%, (e) magnification of (c), (f) the longitudinal view of (b).

## 3. Results and discussion

### 3.1. Characterization of the porous CS monoliths

Porous CS monoliths prepared by unidirectional freeze-drying have oriented pore structures, and their pore size depends on several factors, one of which is the degree of CS cross-linking (Fig. 1). As the amount of cross-linking agent increased, the pore width increased from 50 μm to 100 μm and the length of the pores decreased from 300 μm to 150 μm. These morphology differences are attributed to the changes that occur in the viscosity of the CS solutions with different amounts of cross-linking agent. Since CS is a hydrophilic polymer, it can absorb a large amount of water to form a hydrogel when it comes in contact with water. This ability to absorb water, together interconnected pores, are beneficial for the diffusion of metal ions, which in turn should lead to high adsorption rates for metal ions.

### 3.2. $Q_s$ and Ade at different $Cu^{2+}$ concentrations

The effect of $Cu^{2+}$ concentration on the $Q_s$ and Ade is shown in Fig. 2. For a constant amount of porous CS monolith (0.15 g), the $Q_s$ gradually increased as the initial $Cu^{2+}$ concentration increased until the saturation point was reached at 800 mg/L. At or above this $Cu^{2+}$ concentration a maximum uptake of 141.8 mg/g was obtained. This high adsorption capacity can be attributed to the structure of the adsorbents. CS adsorbents are normally microparticles having a size of about 50 μm. The porous CS monoliths have oriented

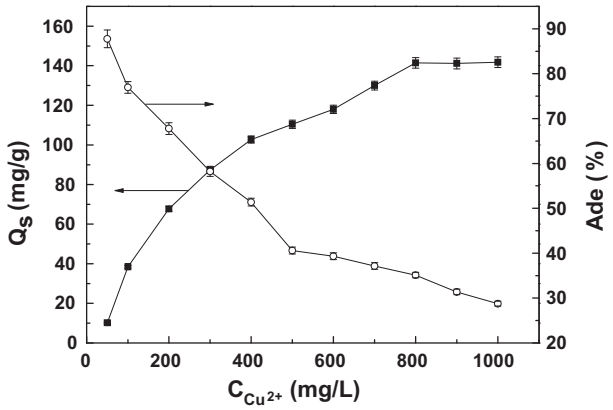


**Fig. 2.** Effect of ion concentration on the $Q_s$ and Ade (0.15% cross-linking agent).

through pore structures (Fig. 1(f)) which are beneficial for the diffusion of metal ions to the surface and interior regions of the porous CS monoliths. The walls of the pores are made of CS plates that have a thickness of about 5 μm, and many "CS micro-ribbons or fibers" protrude from the CS walls (shown in Fig. 1(e)). So the porous CS monoliths have a high surface area which results in more surfacial $-NH_2$ groups for metal ion adsorption, which leads to high $Q_s$. This is why CS is often coated onto particle surfaces to increase the $Q_s$ of CS itself. However the $Q_s$ of the whole adsorbents remains low because the core is usually inert or has a low adsorption capacity [30,44]. The obtained maximum uptake value maybe the highest experimental value to the best of our knowledge [20,30,34]. However, the Ade gradually decreased as the concentration of $Cu^{2+}$ ions in solution increased. These results may be explained by the fact that at high $Cu^{2+}$ concentration, more $Cu^{2+}$ ions are available to adsorb onto the adsorbent, before the adsorption–desorption equilibrium is reached. However, at the same time, at high initial $Cu^{2+}$ concentrations, more $Cu^{2+}$ ions are left in solution simply because the total amount of $Cu^{2+}$ ions is far beyond the $Q_s$ of the porous CS monoliths, which leads to the decline of the Ade.

### 3.3. Adsorption of porous CS monoliths for metal ions

Fig. 3 shows the adsorption behavior for $Cu^{2+}$ when different amounts of porous CS monoliths (different pieces of monoliths with the same size and structure) were used as the adsorbent. For each curve, the Ad increased gradually with time until a saturation plateau was reached. The time needed to reach the maximum adsorption depended on the amount of porous CS. It took 10 h to

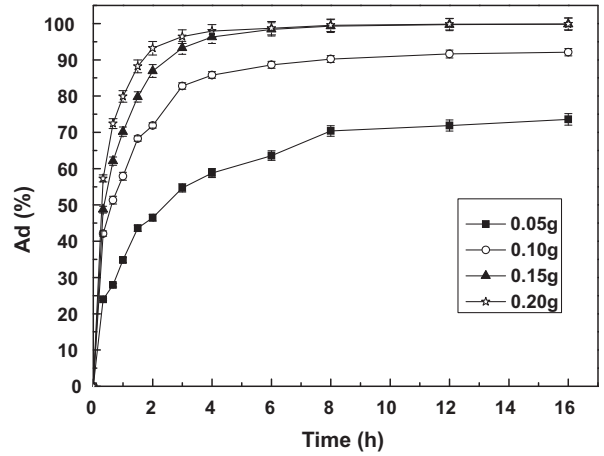


**Fig. 3.** The effect of the CS monolith dosage on the Ad ($Cu^{2+}$: 50 mg/L).

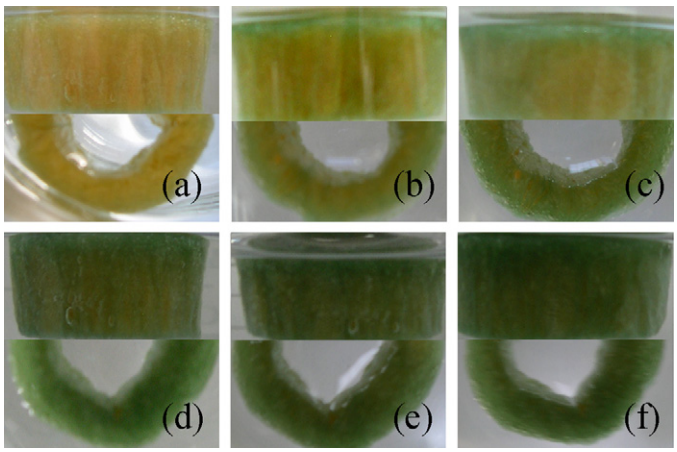


**Fig. 4.** Color change of the porous CS monoliths (side and top views) during the adsorption test (a) 0 min, (b) 20 min, (c) 60 min, (d) 2 h, (e) 4 h, (f) 6 h.

reach the maximum when 0.05 g or 0.10 g porous CS was used, whereas it only took 4 h for 0.2 g porous CS. On the other hand, the Ade increased from about 70% to 99.5% when the amount of porous CS increased from 0.05 g to 0.15 g. A further increase in the amount of adsorbent did not produce any further growth in the Ade. Therefore 0.15 g was adopted as the amount of adsorbent in the subsequent experiments.

The adsorption process can be perceived by the naked eye. As the adsorption process in a 200 mg/L $Cu^{2+}$ solution progressed, the color of the porous CS monoliths gradually changed as shown in Fig. 4. The color of the CS monoliths went from original yellow (Fig. 4(a)), to yellow–green (Fig. 4(b)) and finally to dark green (Fig. 4(f)) as more $Cu^{2+}$ of blue color was adsorbed. From Fig. 4(a–c), it can be observed that the ion adsorption occurred primarily near the surface of the sample during the first 60 min, with the color gradually changing from yellow to lime. After 2 h, the CS monolith turned to green, and after 4 h the entire sample became dark green. The color changes also indicate that the porous CS monoliths were almost saturated after 2 h of adsorption, and reached a maximum adsorption after 4 h. The $Cu^{2+}$ ions were adsorbed by the porous CS monoliths very quickly owing to the highly porous structure of the porous CS monoliths.

### 3.4. The effect of the amount of cross-linking agent on adsorption

The amount of cross-linking agent had a considerable impact on the Ad of the porous CS monoliths for $Cu^{2+}$. This is probably because cross-linking effects both the porosity and the number of available $-NH_2$ groups in the CS monoliths. As shown in Fig. 5, the Ad for $Cu^{2+}$ decreased significantly as the amount of cross-linking agent increased. The adsorption of $Cu^{2+}$ is mainly through the chelation of the metal ion with the amino groups of CS. When the amount of cross-linking agent increased or the reaction time was extended, more amino groups were consumed in the cross-linking reaction with glutaraldehyde which reduces the $Q_t$ for $Cu^{2+}$. Therefore, the amount of cross-linking agent and the cross-linking time need to be carefully controlled during the preparation of porous CS monoliths.

### 3.5. The dependence of Ad on pH

Fig. 6 shows the Ad of the porous CS monoliths at different pH values (adjusted by adding hydrochloric acid). The effect of pH is quite strong and the similar results have also been reported [30,45]. At low pH, the Ad was only 10%, and the value changed little with time. The Ad increased as the pH increased and reached a maximum at pH 6. At lower pH values, the $H^+$ ions in solution compete

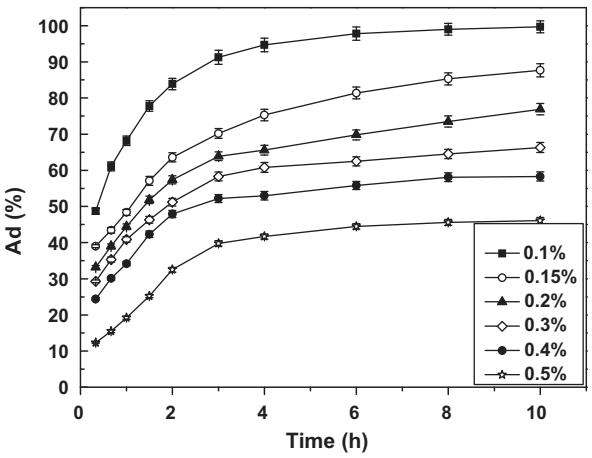


**Fig. 5.** Effect of the amount of cross-linking agent on the Ad ($Cu^{2+}$: 50 mg/L).

with $Cu^{2+}$ for adsorption which leads to reduced $Cu^{2+}$ adsorption. In addition, at low pH, the $-NH_2$ groups on the CS macromolecules become protonated to $NH_3^+$ as shown in Eq. (4). These $-NH_3^+$ cations not only do not chelate with $Cu^{2+}$, but also induce electrostatic repulsions with the $Cu^{2+}$ ions in solution. This hinders the $Cu^{2+}$ ions approach to and coordination with the CS macromolecules. When the pH was above 7.0, flocculation occurred in the $Cu^{2+}$ solution, and above pH 8.0, a precipitation was observed. They are maybe the uncross-linked CS macromolecules that dissolved in the solution and precipitated at high pH.

$$HO - CS - NH_2 \underset{OH^-}{\overset{H^+}{\rightleftharpoons}} HO - CS - NH_3^+ \quad (4)$$

### 3.6. Adsorption of mixed ions

The Ad of the porous CS monoliths for five metal ions in one solution at 20 min, 4 h and 8 h is shown in Fig. 7. The Ad of the monoliths for $Hg^{2+}$ was the highest. Initially, the Ad for $Cu^{2+}$ was lower than that of $Hg^{2+}$, but it increased with time and eventually after 8 h, it reached the same value as $Hg^{2+}$. The Ad of the monoliths for the other three metal ions was similar but much lower than that of $Hg^{2+}$ or $Cu^{2+}$. The Ad sequence for the five metal ions is: $Hg^{2+} > Cu^{2+} > Cd^{2+} > Pb^{2+} > Ni^{2+}$, a trend comparable to that reported by Babel et al. [19].

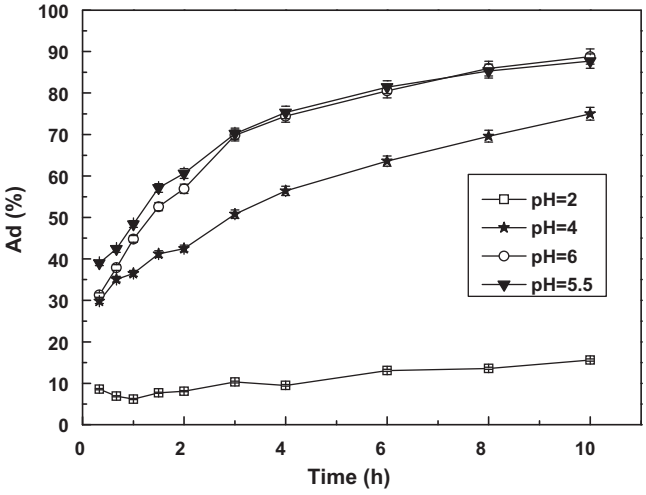


**Fig. 6.** The Ad at different pH values (0.15% cross-linking agent; $Cu^{2+}$: 50 mg/L).

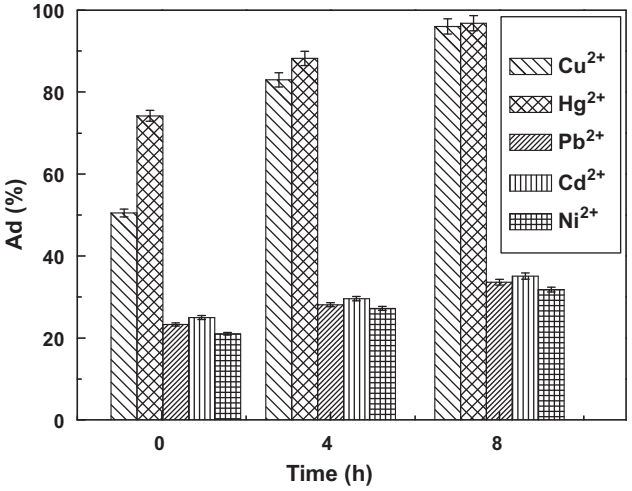


**Fig. 7.** The Ad for different metal ions ($Cu^{2+}$, $Pb^{2+}$, $Hg^{2+}$, $Cd^{2+}$ and $Ni^{2+}$: 50 mg/L).

### 3.7. Improved adsorption by adding EDTA

For the above results, ethanol treated CS monoliths were used to improve the Ade of the monoliths. The ethanol treatment helps to remove the acetic acid that was added during the initial preparation of the monoliths.

Heavy metal ions, such as lead or mercury can be removed from solution by chelation with EDTA, so the addition of EDTA to improve the adsorption of the untreated CS monoliths was also explored. The relationship between Ade and EDTA concentration is shown in Fig. 8. A maximum Ade of 98.35% was achieved for an EDTA concentration of 250 mg/L. The benefit of adding EDTA is significant: the Ade was only 30% when no EDTA was present in the $Cu^{2+}$ solution, whereas it reached over 90% when the EDTA concentration was 250–300 mg/L.

In the presence of EDTA, both the CS macromolecules and the EDTA molecules adsorbed $Cu^{2+}$ through chelation with their $-NH_2$ or –COOH groups. When EDTA is at a relatively low concentration, the –COOH groups of EDTA can interact with the $NH_2$ groups on the CS macromolecules, and thereby allow more $Cu^{2+}$ ions to bond with the CS through this additional CS–EDTA–$Cu^{2+}$ pathway. So the addition of EDTA significantly improves the Ade. However, when excess EDTA is present in the solution, the CS macromolecules cannot offer sufficient $-NH_2$ groups to couple with the EDTA –COOH

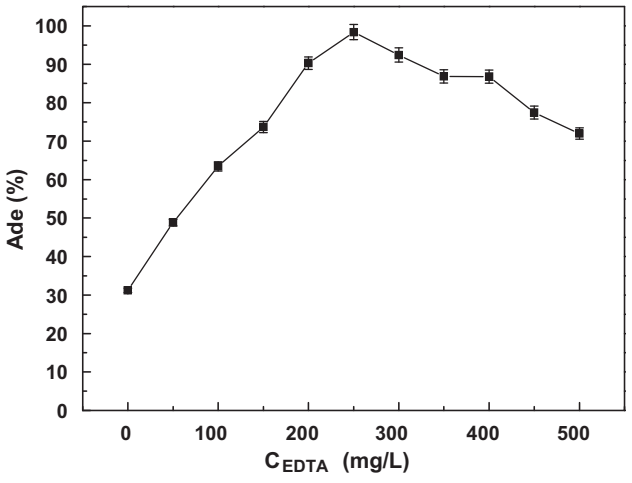


**Fig. 8.** Effect of EDTA concentration on the Ad (0.3% cross-linking agent; $Cu^{2+}$: 100 mg/L).

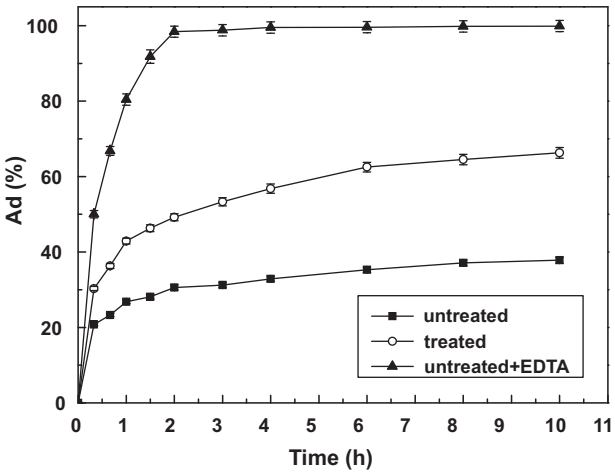


**Fig. 9.** The Ad of different CS monoliths (0.3% cross-linking agent; $Cu^{2+}$: 50 mg/L, EDTA: 200 mg/L).

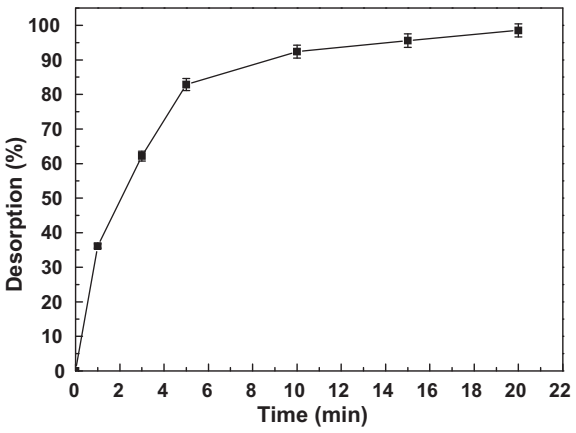


**Fig. 10.** Desorption efficiency of $Cu^{2+}$ from the CS monoliths (0.15% cross-linking agent; $Cu^{2+}$: 50 mg/L).

groups, and a large portion of EDTA molecules are left in solution. Since $Cu^{2+}$ is more likely to chelate with EDTA in solution than with CS, some $Cu^{2+}$ remains in the solution instead of being adsorbed by the CS monoliths, which leads to a loss in Ade.

Fig. 9 compares the Ad of treated and untreated monoliths with and without EDTA. The Ad of the treated CS monoliths was higher than the corresponding untreated ones. Without ethanol treatment, the residual acetic acid in the CS monoliths can protonate the $-NH_2$ groups to $-NH_3^+$ which are then unable to chelate with $Cu^{2+}$. By soaking the monoliths in ethanol to remove the acetic acid, the Ad of the CS monoliths was improved.

After EDTA was added to the $Cu^{2+}$ solution, the untreated monolith showed an increased Ade from 32% to 99.5%, and the time (4–5 h) to reach adsorption equilibrium was also reduced by 2–3 h.

CS and EDTA can both chelate with $Cu^{2+}$. Under acidic conditions, the amino and hydroxyl groups on the CS macromolecules are in the forms of $-NH_3^+$ and $-OH_2^+$, respectively, and therefore the EDTA molecules can be adsorbed by the CS through the electrostatic attractions between these two cations and the EDTA's

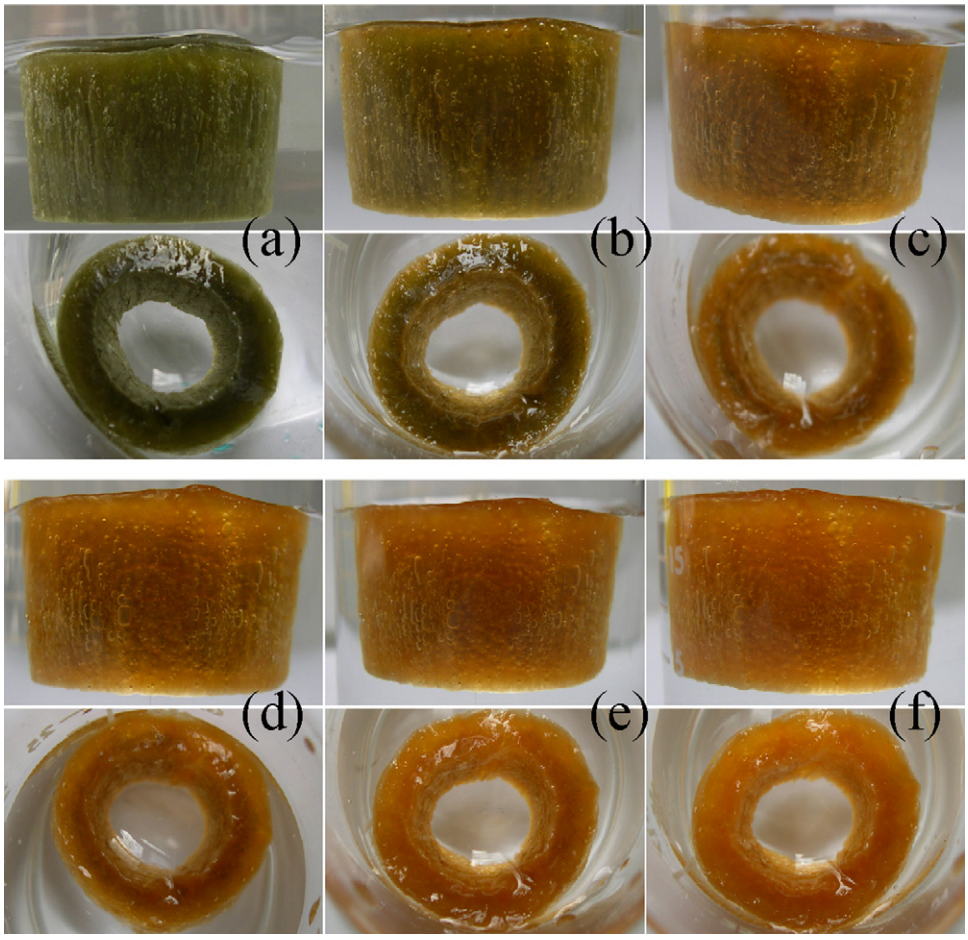


**Fig. 11.** Color change of CS monoliths (side and top views) during desorption of $Cu^{2+}$ (a) 0 min; (b) 1 min; (c) 3 min; (d) 5 min; (e) 10 min; (f) 20 min.

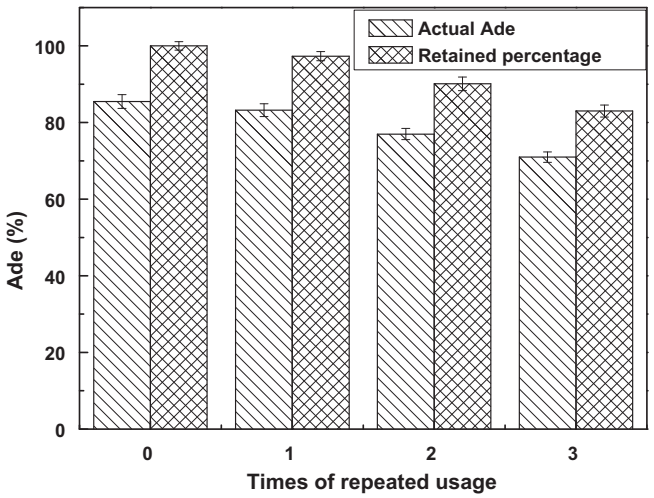


**Fig. 12.** The Ade of the reused monoliths (retained percentage = actual Ade/original Ade × 100) (0.15% cross-linking agent; $Cu^{2+}$: 50 mg/L).

$-COO^-$ groups. The $Cu^{2+}$–EDTA–CS may represent a stronger bonding pathway compared with direct $Cu^{2+}$–CS chelation. Therefore, in the presence of EDTA, untreated CS monoliths can adsorb $Cu^{2+}$ ions with high efficiency through this approach.

### *3.8. Desorption and recycling characteristics of the porous CS monoliths*

The above results show that the porous CS monoliths possess excellent adsorption capabilities for metal ions. But in practice, it is also necessary that such adsorbent materials can be used repeatedly. In this regard, the adsorbed ions need to be readily removed after use. Therefore, the desorption characteristics were studied. Fig. 10 shows the desorption efficiency of $Cu^{2+}$ from the CS monoliths in acidic solution. According to Eq. (4), the amine groups are protonated in acidic solutions, so the electrostatic repulsions between $Cu^{2+}$ and $-NH_3^+$ allow the $Cu^{2+}$ to be easily desorbed from the CS macromolecules.

The desorption of $Cu^{2+}$ from the CS monoliths can also be perceived with the naked eye (Fig. 11). The green CS monolith turned lighter after it was immersed in the acid solution for 1 min because $Cu^{2+}$ ions of blue color were gradually desorbed. After 3 min, the surface of the monoliths became yellow while, the inner part remained green, indicating that the $Cu^{2+}$ had not yet completely desorbed. This phenomenon can be attributed to the lower diffusion rate from the inner part compared to the surface. A similar color gradient also existed in the adsorption process described earlier. After 20 min, the CS monolith returned to its original yellow color, which indicates that the desorption of $Cu^{2+}$ from the porous monoliths was complete.

The Ad of the regenerated CS monoliths was tested and the results are given in Fig. 12. The Ade decreased after regeneration. Nevertheless, they maintained nearly 90% of their original Ade after multiple cycles which indicates the monoliths can be reused. Thus, the porous CS monoliths should be useful for future applications.

## 4. Conclusions

Highly porous CS monoliths with oriented pore structures have been successfully prepared using unidirectional freezing technology. The material shows excellent adsorption performance for a range of heavy metal ions. The Ad is a function of the dosage of CS, pH value, adsorbing time, the amount of cross-linking agent and the amount of EDTA. Under optimum conditions, the high $Q_s$ of 141.8 mg/g for $Cu^{2+}$ can be obtained. Since the porous CS monoliths are biocompatible and biodegradable, and can be easily regenerated after use, they offer a promising environmentally friendly way to treat wastewater containing heavy metal ions.

## Acknowledgements

This work was supported by the National Science Foundation of China (50603017, 50873075) and Tianjin Municipal Science and Technology Commission, PR China (06YFGZGX03000, 09JCZDJC23300).

## References

[1] J.C. Victor, P.X. Ma, Nano-fibrous poly(L-lactic acid) scaffolds with interconnected spherical macropores, Biomaterials 25 (2004) 2065–2073.
[2] H.L. Yun, H.L. Jong, Electrospun dual-porosity structure and biodegradation morphology of montmorillonite reinforced PLLA nanocomposite scaffolds, Biomaterials 26 (2005) 3165–3172.
[3] S.B. Lee, Y.H. Kim, M.S. Chong, Preparation and characteristics of hybrid scaffolds composed of β-chitin and collagen, Biomaterials 25 (2004) 2309–2317.
[4] S.L. Ishaug-Riley, G.M. Kruger, M.J. Yaszemski, Three-dimensional culture of rat calvarial osteoblasts in porous biodegradable polymers, Biomaterials 19 (1998) 1405–1412.
[5] S. Stokols, M.H. Tuszynski, The fabrication and characterization of linearly oriented nerve guidance scaffolds for spinal cord injury, Biomaterials 25 (2004) 5839–5846.
[6] Q. Ao, A.J. Wang, W.L. Cao, C. Zhao, Y.D. Gong, N.M. Zhao, Preparation of porous multi-channeled chitosan conduits for nerve tissue engineering, in: X.D. Zhang, J. Tanaka, Y.T. Yu, Y. Tabata (Eds.), Adv. Biomaterials VI, Trans Tech Publications Inc., Zurich, 2004, pp. 27–30.
[7] J.Y. Wang, Y. Cao, Y. Feng, Multirespensive inverse-opal hydrogels, Adv. Mater. 19 (2007) 3865–3871.
[8] F. Yang, X. Qu, W.J. Cui, J.Z. Bei, F.Y. Yu, S.B. Lu, S.G. Wang, Manufacturing and morphology structure of polylactide-type microtubules orientation-structured scaffolds, Biomaterials 27 (2006) 4923–4933.
[9] M.L. Ferrer, R. Esquembre, I. Ortega, C.R. Mateo, F. del Monte, Freezing of binary colloidal systems for the formation of hierarchy assemblies, Chem. Mater. 18 (2006) 554–559.
[10] H. Zhang, I. Hussain, M. Brust, M.F. Butler, S.P. Rannard, A.I. Cooper, Aligned two- and three-dimensional structures by directional freezing of polymers and nanoparticles, Nat. Mater. 4 (2005) 787–793.
[11] H. Zhang, J. Long, A.I.J. Cooper, Aligned porous materials by directional freezing of solutions in liquid $CO_2$, J. Am. Chem. Soc. 127 (2005) 13482–13483.
[12] M.C. Gutiérrez, M. Jobbágy, N. Rapún, M.L. Ferrer, F. del Monte, A biocompatible bottom-up route for the preparation, Adv. Mater. 18 (2006) 1137–1140.
[13] Y. Shunji, I. Toshiyuki, T. Akio, M. Akira, O. Kazushi, S. Shinichi, S. Kenichi, T. Junzo, Fabrication and mechanical and tissue ingrowth properties of unidirectionally porous hydroxyapatite/collagen composite, Biomed. Mater. Res. 80B (2007) 166–173.
[14] N.A. Carrington, G.H. Thomas, D.L. Rodman, D.B. Beach, Z.L. Xue, Optical determination of Cr(VI) using regenerable, functionalized sol–gel monoliths, Anal. Chim. Acta 581 (2007) 232–240.
[15] T Balaji, S.A. El-Safty, H. Matsunaga, T. Hanaoka, F. Mizukami, Optical sensors based on nanostructured cage materials for the detection of toxic metal ions, Angew. Chem. Int. Ed. 45 (2006) 7202–7208.
[16] P. Barbaro, F. Liguori, Ion exchange resins: catalyst recovery and recycle, Chem. Rev. 109 (2009) 515–529.
[17] S.E. Baker, P.E. Colavita, R.J. Hamers, Functionalized vertically aligned carbon nanofibers as scaffolds for immobilization and electrochemical detection of redox-active proteins, Chem. Mater. 18 (2006) 4415–4422.
[18] Yu Fei Tao, Yue Qiua, Shu Yu Fang, Zhu Yun Liu, Ying Wang, Jian Hua Zhua, Trapping the lead ion in multi-components aqueous solution by natural clinoptilolite, J. Hazard. Mater. 180 (2010) 282–288.
[19] S. Babel, T.A. Kumiawan, Low-cost adsorbents for heavy metals uptake from contaminated water, J. Hazard. Mater. 97 (2003) 219–243.
[20] K.H. Chu, Removal of copper from aqueous solution by chitosan in prawn shell: adsorption equilibrium and kinetics, J. Hazard. Mater. B90 (2002) 77–95.
[21] W.S.W. Ngah, S.A. Ghani, A. Kamari, Adsorption behaviour of Fe(II) and Fe(III) ions in aqueous solution on chitosan and cross-linked chitosan beads, Bioresour. Technol. 96 (2005) 443–450.
[22] W.S.W. Ngah, S. Fatinathan, Chitosan flakes and chitosan-GLA beads for adsorption of *p*-nitrophenol in aqueous solution, Colloids Surf. A: Physicochem. Eng. Aspects 277 (2006) 214–222.
[23] A.H. Chen, S.C. Liu, C.Y. Chen, C.Y. Chen, Comparative adsorption of Cu(II), Zn(II), and Pb(II) ions in aqueous solution on the crosslinked chitosan with epichlorohydrin, J. Hazard. Mater. 154 (2008) 184–191.
[24] W.S.W. Ngah, C.S. Endud, R. Mayanar, Removal of copper(II) ions from aqueous solution onto chitosan and cross-linking chitosan beads, React. Funct. Polym. 20 (2002) 181–190.
[25] E. Guibal, Interactions of metal ions with chitosan-based sorbents: a review, Sep. Purif. Technol. 38 (2004) 43–74.

[26] P.O. Osifo, A. Webster, H. van der Merwe, H.W.J.P. Neomagus, M.A. van der Gun, D.M. Grant, The influence of the degree of cross-linking on the adsorption properties of chitosan beads, Bioresour. Technol. 99 (2008) 7377–7382.
[27] V.M. Boddu, K. Abburi, J.L. Talbott, E.D. Smith, R. Haasch, Removal of arsenic (III) and arsenic (V) from aqueous medium using chitosan-coated biosorbent, Water Res. 42 (2008) 633–642.
[28] A. Gupta, V.S. Chauhan, N. Sankararamakrishnan, Preparation and evaluation of iron-chitosan composites for removal of As(III) and As(V) from arsenic contaminated real life groundwater, Water Res. 43 (2009) 3862–3870.
[29] K. Swayampakula, V.M. Boddu, S.K. Nadavala, K. Abburi, Competitive adsorption of Cu (II), Co (II) and Ni (II) from their binary and tertiary aqueous solutions using chitosan-coated perlite beads as biosorbent, J. Hazard. Mater. 170 (2009) 680–689.
[30] S. Hasan, T.K. Ghosh, D.S. Viswanath, V.M. Boddu, Dispersion of chitosan on perlite for enhancement of copper(II) adsorption capacity, J. Hazard. Mater. 152 (2008) 826–837.
[31] H. Ghassabzadeha, A. Mohadespour, M. Torab-Mostaedi, P. Zaheri, M.G. Maragheh, H. Taheri, Adsorption of Ag, Cu and Hg from aqueous solutions using expanded perlite, J. Hazard. Mater. 177 (2010) 950–955.
[32] L. Wang, R. Xing, S. Liu, Y. Qin, K. Li, H. Yu, R.F. Li, P.C. Li, Studies on adsorption behavior of Pb(II) onto a thiourea-modified chitosan resin with Pb(II) as template, Carbohydr. Polym. 81 (2010) 305–310.
[33] L.M. Zhou, Y.P. Wang, Z.R. Liu, Q.W. Huang, Characteristics of equilibrium, kinetics studies for adsorption of Hg(II), Cu(II), and Ni(II) ions by thiourea-modified magnetic chitosan microspheres, J. Hazard. Mater. 161 (2009) 995–1002.
[34] E. Repoa, J.K. Warchol, T.A. Kurniawan, M.E.T. Sillanpaa, Adsorption of Co(II) and Ni(II) by EDTA- and/or DTPA-modified chitosan: kinetic and equilibrium modeling, Chem. Eng. J. 161 (2010) 73–82.
[35] A. Kamaria, W.S.W. Ngah, Isotherm, kinetic and thermodynamic studies of lead and copper uptake by $H_2SO_4$ modified chitosan, Colloids Surf. B: Biointerfaces 73 (2009) 257–266.
[36] H.L. Vasconcelos, V.T. Fa′vere, N.S. Goncalves, M.C.M. Laranjeira, Chitosan modified with Reactive Blue 2 dye on adsorption equilibrium of Cu(II) and Ni(II) ions, React. Funct. Polym. 67 (2007) 1052–1060.
[37] Y.T. Zhou, H.L. Nie, C. Branford-White, Z.Y. He, L.M. Zhu, Removal of $Cu^{2+}$ from aqueous solution by chitosan-coated magnetic nanoparticles modified with $\alpha$-ketoglutaric acid, J. Colloid Interface Sci. 330 (2009) 29–37.
[38] B. Kannamba, K. Laxma Reddy, B.V. Appa Rao, Removal of Cu(II) from aqueous solutions using chemically modified chitosan, J. Hazard. Mater. 175 (2010) 939–948.
[39] X.H. Wu, Y. Liu, X. Li, Preparation of aligned porous gelatin scaffolds by unidirectional freeze-drying method, Acta Biomater. 6 (2010) 1167–1177.
[40] A. Abarrategi, M.C. Gutiérrez, C. Moreno-Vicente, M.J. Hortiguela, V. Ramos, J.L. López-Lacomba, M.L. Ferrer, F. del Monte, Multiwall carbon nanotube scaffolds for tissue engineering purposes, Biomaterials 29 (2008) 94–102.
[41] X. Wu, Y. Liu, X. Li, P. Wen, Y. Zhang, Y. Long, X. Wang, Y. Guo, F. Xing, J. Gao, Preparation of aligned porous gelatin scaffolds by unidirectional freeze-drying method, Acta Biomater. 6 (2010) 1167–1177.
[42] M. Renli, V.M. Willy, A. Freddy, Determination of cadmium, copper and lead in environmental samples: an evaluation of flow injection online sorbent extraction for flame atomic absorption spectrometry, Anal. Chim. Acta 285 (1994) 33–43.
[43] P.C. Li, S.J. Jiang, Electrothermal vaporization inductively coupled plasma-mass spectrometry for the determination of Cr, Cu, Cd, Hg and Pb in rice flour, Anal. Chim. Acta 495 (2003) 143–150.
[44] M.W. Wan, C.C. Kan, B.D. Rogel, M.L.P. Dalida, Adsorption of copper (II) and lead (II) ions from aqueous solution on chitosan-coated sand, Carbohydr. Polym. 80 (2010) 891–899.
[45] R. Laus, T.G. Costa, B. Szpoganicz, V.T. Favere, Adsorption and desorption of Cu(II), Cd(II) and Pb(II) ions using chitosan crosslinked with epichlorohydrin-triphosphate as the adsorbent, J. Hazard. Mater. 183 (2010) 233–241.